iScience

Article

Cell-intrinsic regulation of HBV RNAs by the nonsense-mediated mRNA decay pathway controls viral replication

Graphical abstract

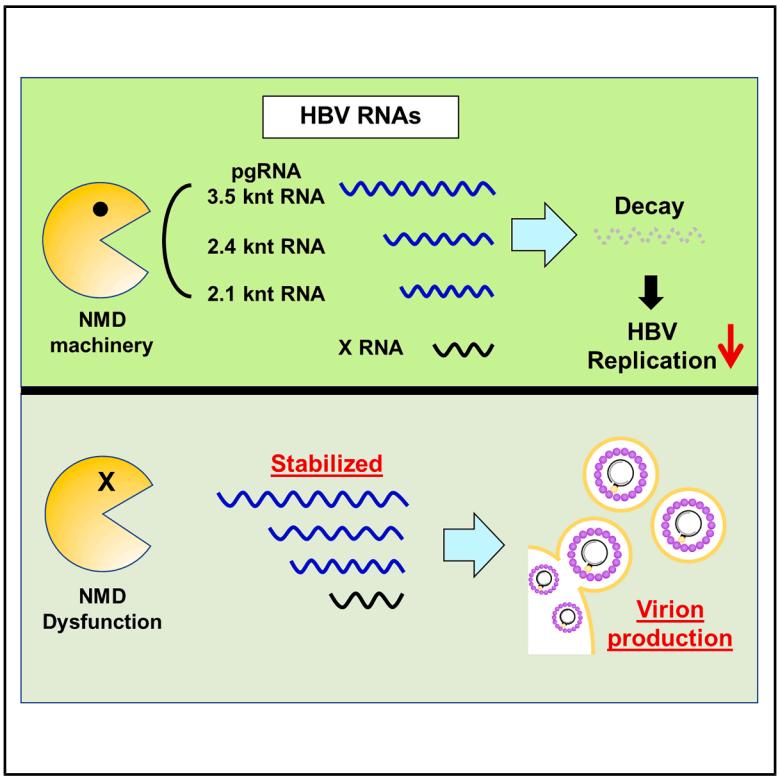

Highlights

- NMD pathway targets HBV RNAs such as pgRNA, 2.4 knt RNA, and 2.1 knt RNA
- Stability of HBV RNAs contributes efficient HBV replication
- NMD pathway governs HBV infection as an intrinsic antiviral defense

Authors

Masami Wada, Chiharu Morita, Eriko Ohsaki, Keiji Ueda

Correspondence

mawada@virus.med.osaka-u.ac.jp (M.W.), kueda@virus.med.osaka-u.ac.jp (K.U.)

In brief

Molecular biology; Cell biology; Genomics

Wada et al., 2025, iScience *28*, 112460
May 16, 2025
https://doi.org/10.1016/j.isci.2025.112460

CellPress

iScience

CellPress
OPEN ACCESS

Article

Cell-intrinsic regulation of HBV RNAs by the nonsense-mediated mRNA decay pathway controls viral replication

Masami Wada,[1,2,*] Chiharu Morita,[1] Eriko Ohsaki,[1] and Keiji Ueda[1,*]
[1]Division of Virology, Department of Microbiology and Immunology, Osaka University Graduate School of Medicine, 2-2 Yamada-oka, Suita, Osaka 565-0871, Japan
[2]Lead contact
*Correspondence: mawada@virus.med.osaka-u.ac.jp (M.W.), kueda@virus.med.osaka-u.ac.jp (K.U.)
https://doi.org/10.1016/j.isci.2025.112460

SUMMARY

Hepatitis B virus (HBV) is a causative agent for chronic liver hepatitis, which confers risk for liver cirrhosis and hepatocellular carcinoma. Among key viral transcripts, HBV pregenome RNA (pgRNA) is indispensable for viral replication, and therefore, quality control of pgRNA is critical for the HBV life cycle. Here, we revealed degradation of HBV RNAs by the nonsense-mediated mRNA decay (NMD) pathway, a host surveillance system of RNA quality. Degradation kinetics of the HBV RNAs indicated that pgRNA, 2.4 knt RNA, and 2.1 knt RNA were targets of the NMD pathway and also interacted robustly with phosphorylated UPF1 but not X RNA. Northern blotting showed that decay of the viral NMD candidates was also delayed in NMD-deficient cells. In contrast, NMD depletion promoted the formation of capsids containing genomic DNA and exhibiting antigen production. Our data strongly suggest that the NMD pathway inspects HBV transcripts to regulate HBV replication as an intrinsic antiviral defense.

INTRODUCTION

Hepatitis B virus (HBV) is an etiological agent for chronic hepatitis, and HBV-infected individuals have high risks of lethal cirrhosis and hepatocellular carcinoma (HCC).[1,2] The current therapeutics against HBV, such as nucleoside analogs and peg-interferon, cannot induce complete HBV remission because of the lifelong medication and the drug-escape mutants, and they also have serious side effects. Therefore, the development of a more efficient HBV treatment is urgently required.

HBV is a small DNA virus whose genome is 3.2 kb long and is a partially double stranded, relaxed circular DNA (rcDNA). There are mainly four kinds of overlapping genes that respectively encode a precore/core protein, polymerase, three HBV surface proteins, and the X protein. In the life cycle, HBV genomic rcDNA is released into the nucleus after entering cells and converted into covalently closed circular DNA (cccDNA). cccDNA is transcription competent and produces four main viral RNAs: pregenome RNA (pgRNA)/3.5 k nucleotide (nt) RNA as a template for reverse transcription and pre-core/core proteins and polymerase; 2.4 knt/2.1 knt RNA for large S, medium S, and small S (SS or simply HBs) proteins; and X RNA (0.7 knt).[3,4] pgRNA in particular plays a crucial role as a template of reverse transcription associated with HBV replication.

Although many viruses struggle to establish infection and produce progeny viruses, they are monitored by cellular sensing systems such as pattern-recognition receptors (PRRs) at the entry step.[5,6] Viral nucleic acids—either RNAs or DNAs generated during viral transcription and replication—are typical pathogen-associated molecular patterns recognized by cellular PRRs including Toll-like receptors, retinoic acid-inducible-I-like receptors, melanoma differentiation-associated gene 5, OTU deubiquitinase 3 (OTUD3), and cytosolic cyclic GMP-AMP synthase-stimulator of interferon genes (STING) DNA sensors that lead to induction of immunity against viral infection.[5–8] As for HBV, its infection has also been reported to be monitored by such systems.[9,10]

The nonsense-mediated mRNA decay (NMD) pathway is another means of intrinsic innate immunity against viruses and works as an mRNA surveillance system to control the mRNA quality and thereby maintain the intracellular environment[11] (Figure 1A). NMD is activated by ribosomal arrest at an unexpected position such as a premature termination codon (PTC) on the transcripts. Mechanistically, NMD works on mRNAs during the first round of translation initiated by eIF4F.[12–14] Exon junction complexes (EJCs) formed by post-host splicing of pre-mRNAs are normally removed during host translation. On the other hand, due to PTC on aberrant transcripts, the remaining EJCs play critical roles for the recognition of NMD substrates and the promotion of RNA degradation.[15,16] Among NMD factors such as upstream-shift proteins (UPF1, 2, and 3), UPF1 in particular is indispensable to govern the NMD pathway and transmit the NMD-associated PI3K-related kinase

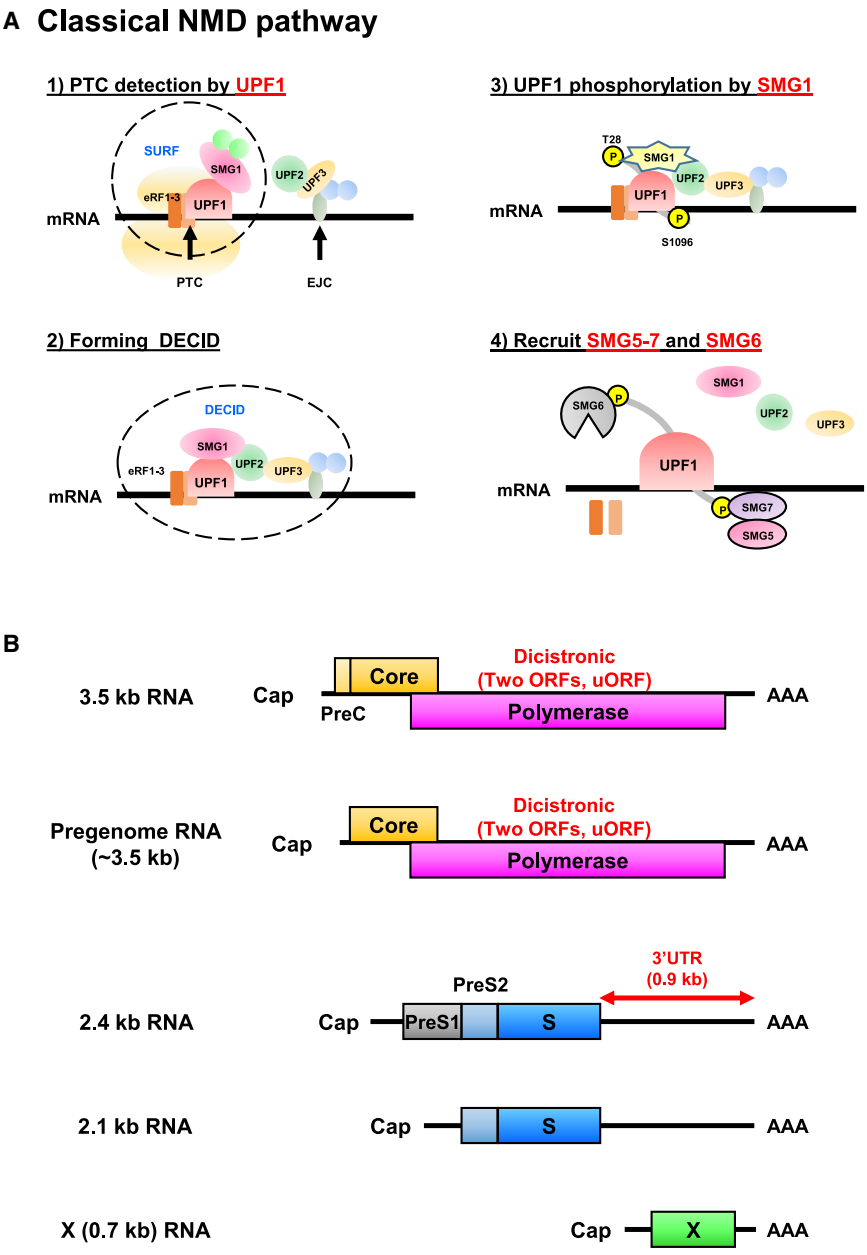

Figure 1. Classical NMD pathway and schematic HBV transcripts harboring NMD-inducing features

(A) Classical NMD pathway are schematically represented.

(B) Major HBV transcripts are schematically represented. Markable NMD-inducing features in their transcripts are shown (dicitronic [two ORFs, uORF], long 3′ UTR).

SMG1 by UPF1 phosphorylation to execute endonucleolysis and exonucleolysis of the aberrant transcripts by the recruitment of the SMG6 and SMG5–7 complex, respectively.[11,17] In addition to typical NMD substrates such as PTC, NMD targets such as multiple open reading frame (ORFs) and upstream ORF (uORF)- and long 3′ untranslated region (UTR)-containing transcripts have been shown to trigger RNA degradation in an EJC-independent manner.[18]

Recent studies have suggested that virus-related RNAs such as Semliki Forest virus,[19] hepatitis C (HCV),[20] Zika virus (ZIKV),[21] the coronavirus murine hepatitis virus (MHV),[22] and Kaposi's sarcoma-associated herpesvirus (KSHV)[23] are likely to promote NMD because they possess one or more unique features targeting the NMD pathway in their genome or transcripts.[19,22–25] Thus, NMD could be recognized as a cell-intrinsic contributor to antiviral immunity.

In the case of HBV, there is little information regarding the mechanism by which HBV RNAs are monitored in the cell. Therefore, elucidation of the HBV RNA inspection system within cells would be expected to promote the further development of HBV treatments. Here, we showed that HBV pgRNA/3.5 knt RNA, 2.4 knt RNA, and 2.1 knt RNA carrying NMD-inducing features were degraded by an UPF1-mediated NMD pathway but X RNA was not. We further proposed that the NMD pathway restricted the early and late HBV infection cycle by targeting HBV RNAs in hepatocytes. Thus, our data strongly suggest that the NMD pathway plays an important role in cell-intrinsic antiviral activity via decay of HBV transcripts, leading to reduction of HBV genomes.

RESULTS

The NMD pathway targets HBV RNAs for rapid decay, with the exception of X RNA

We considered that HBV RNAs may be candidates for targeting by the NMD pathway because pgRNA or 3.5 knt transcripts are dicistronic RNA, and 2.4 knt or 2.1 knt transcripts have long 3′ UTRs that would make them suitable NMD targets[18] (Figure 1B). To test our hypothesis that major HBV RNAs except X RNA are recognized by the NMD pathway, we first examined changes to the NMD pathway following knockdown of NMD pathway-related factors such as UPF1 and 2 (Figure S1). We prepared four HBV RNA transcripts of pgRNA, 2.4 knt RNA, 2.1 knt RNA, and X RNA (~0.7 knt) by *in vitro* transcription with capped and poly A-tailed RNA and transfected them into 293T cells. After 1 h absorption by RNA transfection, the degradation kinetics of each HBV RNA was monitored while knocking down UPF1 and UPF2. Under NMD cessation by small interfering RNA (siRNA)-mediated knockdown of UPF1 or UPF2 in 293T cells (see Figure 4A), the

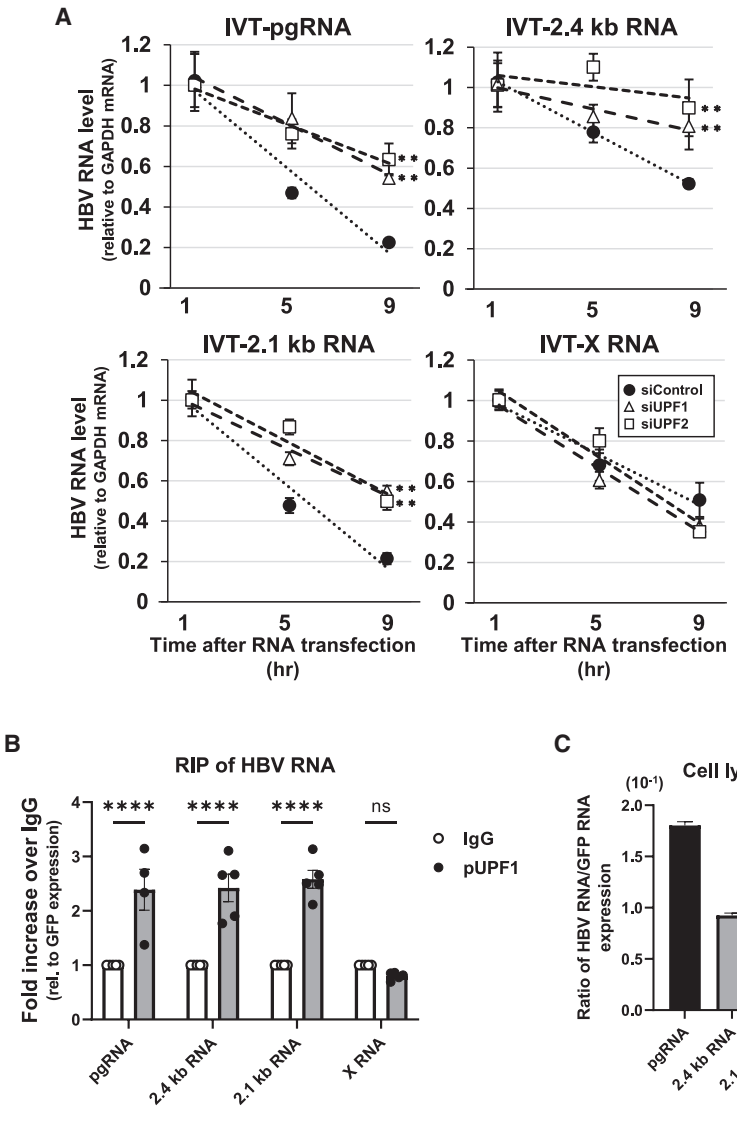

Figure 2. HBV transcripts are targeted by NMD through UPF1 recognition in 293T cells

(A) Degradation kinetics of major HBV transcripts. HEK293T cells were transfected with *in vitro*-transcribed (IVT-) HBV RNA, pgRNA RNA, 2.4 knt RNA, 2.1 knt RNA, or X RNA, and each RNA level was chased with RT-qPCR every 4 h up to 8 h h post transfection. Data are shown as ratios relative to the amount of cellular GAPDH mRNA, which was also determined by RT-qPCR.

(B) RNA immunoprecipitation (RIP) with an anti-pUPF1 antibody. HEK293T cells were transfected with IVT-HBV RNA as described in the main text. Co-transfected IVT-GFP mRNA was used as an internal control. Subsequently, pUPF1-bound RNA was isolated with an anti-pUPF1 antibody, followed by RT-qPCR using a primer set for HBV RNAs and GFP mRNA. Data of HBV RNA precipitation are shown as ratios relative to co-precipitated GFP mRNA in each RIP experiment.

(C) Intracellular HBV RNAs 1 h after RNA transfection. Data of input HBV RNAs are shown as ratios relative to intracellular GFP mRNA amounts. The data are presented as means with standard error of the mean (SEM) of at least three independent experiments. Statistical analysis was done by one-way ANOVA with Dunnett's multiple comparisons test or two-way ANOVA with Sidak's multiple comparisons test.

amounts of transfected HBV RNAs were measured by quantitative reverse-transcription PCR (RT-qPCR) at the indicated time points. We found that the decay of *in vitro* transcribed (IVT)-pgRNA transfected into 293T cells was significantly delayed by depletion of UPF1, a key mediator of the NMD pathway (Figure 2A), along with the IVT-2.4 knt and -2.1 knt HBV RNAs (Figure 2A). Furthermore, depletion of UPF2, which is an EJC component related to NMD, also led to slow degradation of pgRNA, 2.4 knt RNA, and 2.1 knt RNA but not X RNA (Figure 2A). Because NMD needs UPF1 to recognize RNA, we tested whether UPF1 interacted with HBV RNAs. We performed RNA immunoprecipitation (RNA-IP) with an anti-phosphorylated UPF1 (pUPF1) antibody, which can precipitate alternative ribosomal-like protein 3 (rpL3) mRNA, which is an endogenous NMD target,[26] but not vault RNA1-1 (vtRNA), which is a small non-coding RNA not recognized by UPF1 (Figure S2). We found that pUPF1 strongly interacted with pgRNA, 2.4 knt RNA, and 2.1 knt RNA but much less with X RNA, compared to IVT GFP mRNA as a negative control (Figure 2B), while each viral transcript was comparably transfected (Figure 2C).

To further understand the degradation kinetics of HBV RNAs, we adopted a different approach by pulse-chase using a tetracycline (Tet)-regulated HBV-producing cell line, HepAD38.7, in which HBV production was induced by withdrawal of Tet[27]; we also used an siRNA against SMG6, a downstream factor of the NMD pathway. The results showed that each factor was well knocked down by the respective siRNA (Figure 3A). In this case, it was expected that both pgRNA and 3.5 knt RNA would be produced upon Tet removal in HepAD38.7 cells. However, the pgRNA/3.5knt RNA accumulated by Tet removal was more slowly degraded in NMD-deficient cells after adding either Tet or actinomycin D to the medium (Figures 3B and S3A, respectively). Chemical inhibition of the NMD pathway using the NMD inhibitors wortmannin and cycloheximide delayed the degradation of accumulated pgRNA (Figure S3B). In addition, northern blotting clearly showed delayed degradation kinetics of 2.4 and 2.1 knt RNA as well as pgRNA/3.5 knt RNA in NMD-deficient cells, while we could not evaluate X mRNA degradation, since X mRNA was expressed at low levels in the cells (Figure 3C). RNA-IP with an antibody against pUPF1 showed significant interaction of pgRNA with pUPF1 in HBV-replicating cells as well as rpL3 mRNA but not vtRNA (Figure 3D), compared to a

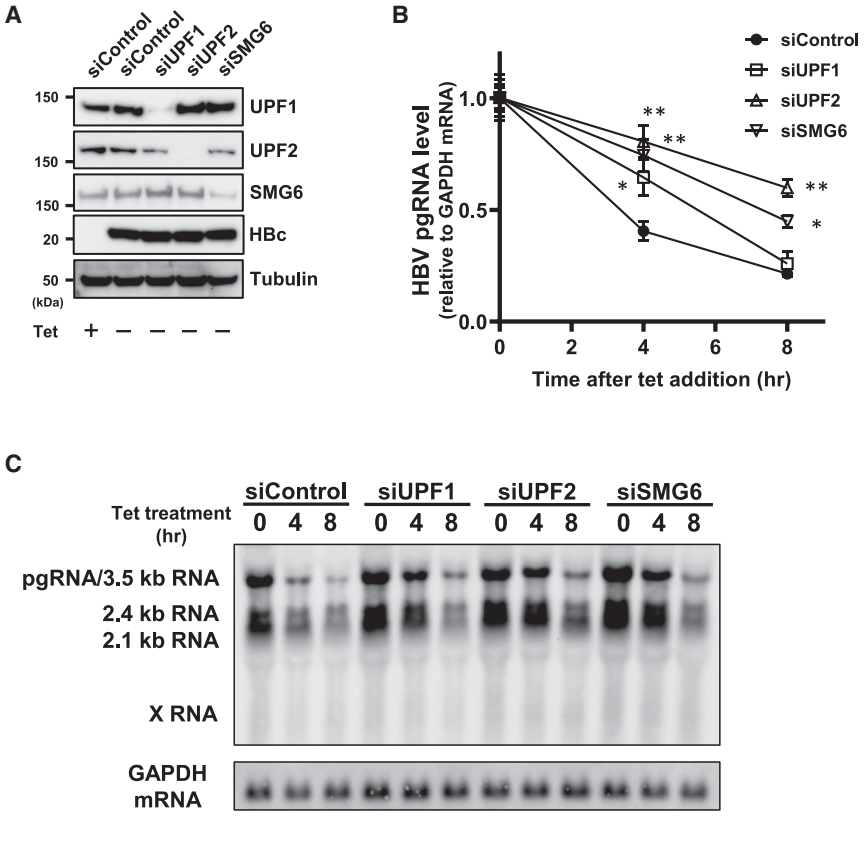

Figure 3. HBV transcripts are targeted by NMD through UPF1 recognition in HBV-replicating cells (HepAD38.7)

(A) Protein levels of NMD factors. The protein level was monitored in HepAD38.7 cells treated with each siRNA after 72 h HBV induction. The HBV induction was also assessed by HBc expression with western blot.

(B) Degradation kinetics of pgRNA/3.5 knt RNA. Intracellularly accumulated pgRNA/3.5 knt RNA by Tet removal was measured with RT-qPCR every 2 h for 8 h after re-addition of Tet. The GAPDH mRNA level was also monitored with RT-qPCR. Data are shown as the ratio of pgRNA/3.5 knt RNA to GAPDH.

(C) Northern blotting analysis of HBV-related transcripts in NMD-depleted HepAD38.7 cells. Total RNA was extracted and separated on an agarose gel under a denaturing condition. HBV-related transcripts or GAPDH mRNA was detected by the corresponding probe.

(D) RNA immunoprecipitation (RIP) using an anti-pUPF1 antibody followed by RT-qPCR. The pUPF1-bound RNAs were isolated and then RT-qPCR analyses were conducted for pgRNA/3.5 knt RNA, vtRNA1-1, and alternative rpL3 mRNA. Data are presented as the fold increase over normal IgG-bound RNA in each target gene, or as mean values with SEM of at least three independent experiments.

Statistical analysis was done by one-way ANOVA with Dunnett's multiple comparisons test or two-way ANOVA with Sidak's multiple comparisons test.

control IgG. Together, these data suggest that HBV mRNAs except X RNA are substrates of the NMD pathway for rapid decay.

The NMD pathway restricts HBV core encapsidation of pgRNA and reverse transcription in pgRNA-transfected cells

Having confirmed that pgRNA/3.5 knt RNA is a likely target of the NMD pathway, we next investigated whether inhibition of pgRNA decay by NMD depletion would induce the efficient formation of encapsidated HBV DNA in the presence of siRNA to knock down NMD pathway-related factors (Figure 4A). Theoretically, because pgRNA encodes the core protein and polymerase and functions as a template for reverse transcription, encapsidated HBV DNA should be detectable in *in vitro* transcribed (IVT)-pgRNA-transfected cells (Figure 1B). Three days after transfecting IVT-pgRNA into 293T cells, we measured the expression of HBeAg in 293T cells and also tried to detect encapsidated HBV DNA reverse-transcribed from IVT-pgRNA in the cells.

We checked the expression levels of intracellular core protein in NMD-depleted cells by co-transfection with both IVT-pgRNA and IVT-GFP RNA. GFP expression was comparable in all cells, and siRNA effectively knocked down each NMD pathway-related protein (Figure 4A). The HBc protein appeared to be expressed more highly in siUPF1- and siUPF2-treated cells compared to siControl-treated cells (Figure 4A). Accordingly, HBeAg ELISA that can detect intracellular HBc protein showed greater expression of the HBeAg and HBc protein in such cells when the NMD factors were knocked down (Figure 4B), and so did encapsidated HBV DNA (Figure 4C), while pgRNA with a mutation of pol gene that resulted in a loss of reverse-transcription activity (pol dead) could not produce the encapsidated HBV DNA (Figure S4A, left), even though HBeAg was comparably

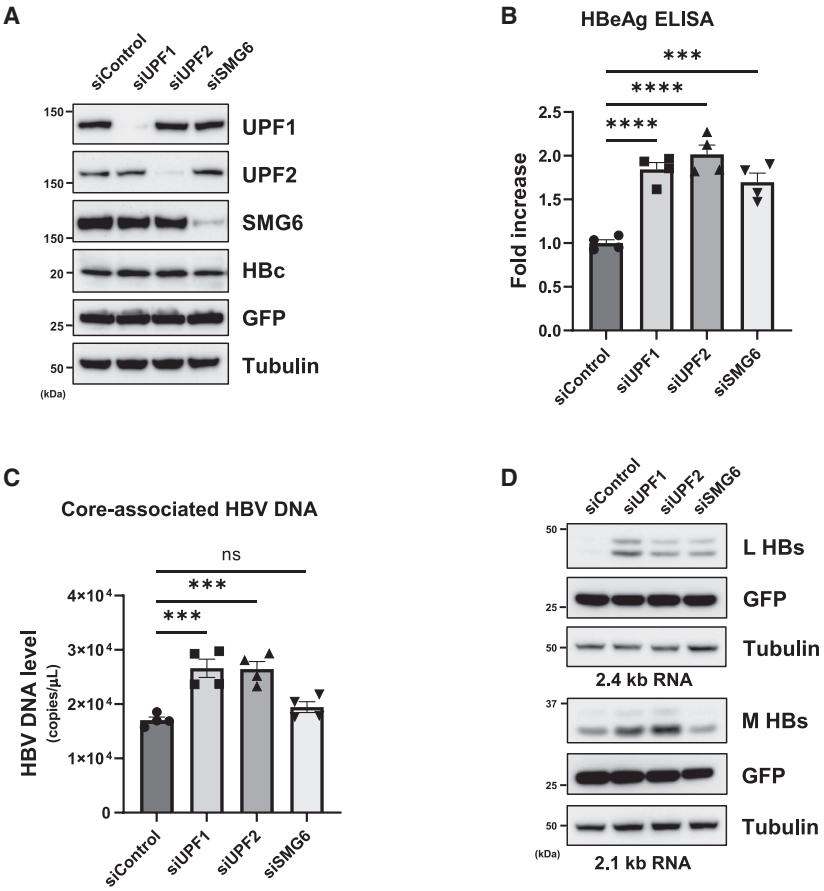

Figure 4. The NMD pathway regulates encapsidation of pgRNA in HEK293T cells

(A) Protein levels of NMD factors in siRNA-mediated knockdown HEK293T cells. Each siRNA was co-transfected with each of IVT-pgRNA, IVT-Renilla luciferase (rLuc) mRNA, and IVT-GFP mRNA. HBc proteins and GFP were monitored as transfection controls and tubulin as an internal control, and detected using the appropriate antibodies.

(B) HBeAg and HBc protein in the transfected cell lysates was measured by HBeAg ELISA. The data were normalized by rLuc activity and shown as fold ratios to siControl-transfected cells.

(C) Encapsidated core-associated HBV DNA from transfected pgRNA in NMD-depleted HEK293T cells was quantified by qPCR. The data were normalized by rLuc activity.

(D and E) Protein levels of HBs preS1 (L HBs) and preS2 (M HBs) antigens in cell lysates of IVT-2.4 or 2.1 knt RNA-transfected HEK293T cells were detected by immunoblot (D) and ELISA (E). ELISA data were normalized by rLuc activity.

(F) NMD-depleted HEK293T cells were co-transfected with IVT-2.4 knt RNA, 2.1 knt RNA, small S RNA, and rLuc mRNA. The culture media were subjected to ELISA at 72 h post RNA transfection. Each absorbance of 450 nm was normalized by rLuc activity.

The data are represented as mean values relative to the siControl with SEM of at least three independent experiments. Statistical analysis was done by one-way ANOVA with Dunnett's multiple comparisons test.

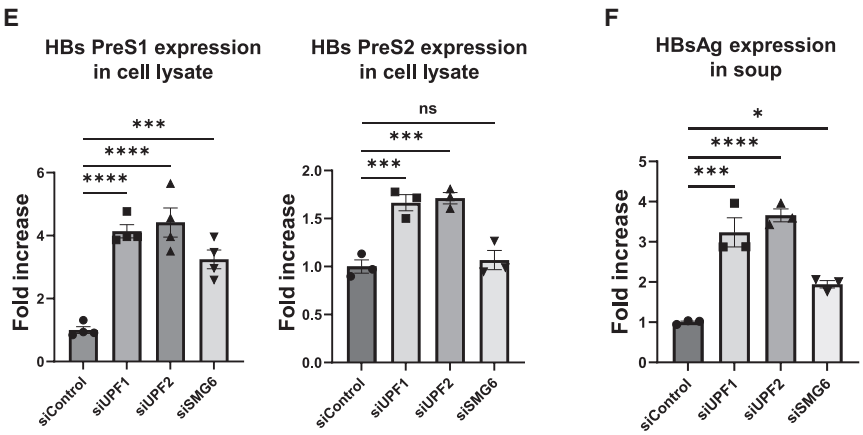

detected (Figure S4A, right). Consistent with the above, an immunofluorescence assay showed that HBc levels were especially elevated in UPF1-, UFP2-, and SMG6-depleted cells (Figure S4B). Taken together, these data suggested that HBV pgRNA is inspected and controlled by the NMD system.

Because the 2.4 and 2.1 knt RNAs encoding large (L), medium (M), and small (S) HBs envelop proteins that carry long 3′ UTRs, we next examined whether these transcripts were also monitored by the NMD system. For this purpose, we directly transfected either IVT-2.4 or IVT-2.1 knt RNA into NMD-depleted 293T cells. Western blotting and ELISA data showed that intracellular expression of L-HB and M-HB proteins was enhanced in NMD-depleted 293T cells transfected with either 2.4 or 2.1 knt RNA carrying long 3′ UTR transcripts, especially in UPF1 and UPF2 knocked-down cells (Figures 4D and 4E). We further examine the extracellular expression of HBs by employing non-authentic IVT-small S RNA encoding only S HBs, which has a comparable 3′ UTR, because no expression of S HBs was observed in 293T cells transfected with IVT-2.4 and 2.1 knt RNA (Figure S4C), resulting in no secretion of HBs in soup. We found that HBsAg was successfully expressed in soup by transfection with 2.4 knt, 2.1 knt, and small S RNA and was also increased in UPF1 or UPF2 knockdown cells (Figure 4F), though siSMG6 did have less or slight of an effect in this case, especially for preS2 expression. Nonetheless, these data suggested that the NMD pathway is involved in the stability of HBV transcripts and later affects the antigen expression.

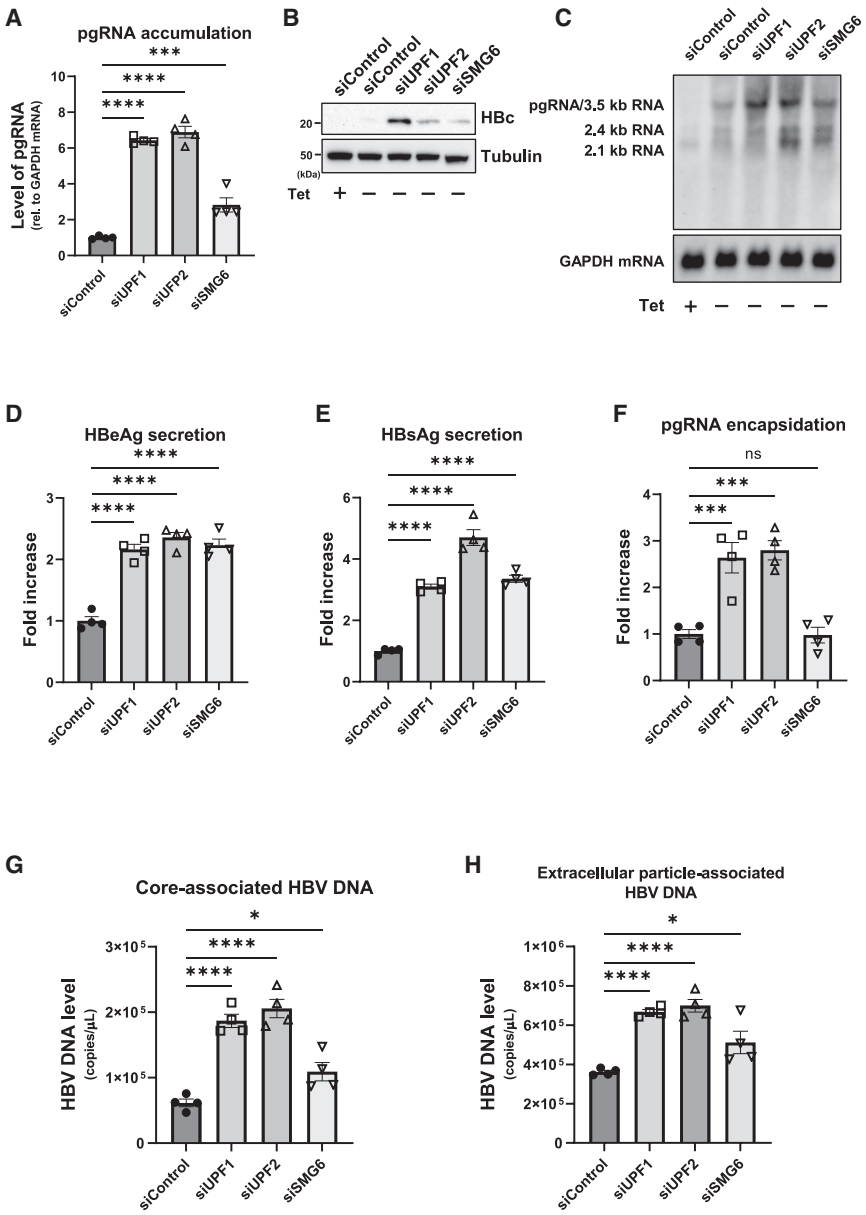

Figure 5. The NMD pathway negatively controls HBV replication in HBV-replicating cells (HepAD38.7)

(A) The levels of pgRNA/3.5 knt RNA expression were determined by RT-qPCR in HBV-replicating cells with depletion of NMD factors at 72 h post Tet removal. The expression levels were normalized by the level of GAPDH mRNA.

(B) Protein level of HBc was monitored in HepAD38.7 cells treated with each siRNA after 48 h HBV induction.

(C) Intracellular pgRNA/3.5 knt RNA, 2.4 knt, and 2.1 knt RNA were detected by northern blotting using specific probes in NMD factor-depleted HBV-replicating cells.

(D and E) HBeAg and HBsAg in the culture medium. Medium was collected from the cells, and HBeAg (D) and HBsAg (E) were measured with ELISA. The OD values were normalized by total protein levels, and the data are shown as the fold increase over the values of siControl-transfected cells.

(F) Level of encapsidated pgRNA. Lysates of the treated cells were prepared in a hypotonic buffer. After degrading nucleic acids outside the intracellular particles, encapsidated pgRNAs were extracted and the amount was measured by RT-qPCR. The data were shown as fold increase to the value of siControl-transfected cells.

(G) Amount of core-associated HBV DNA. Core particle-associated DNA was extracted and then measured by qPCR.

(H) Amount of extracellular particle-associated HBV DNA. Secreted HBV particles were precipitated with 6% PEG8000, and nucleic acids outside the particles were degraded as described in the main text. Then, the particle-associated HBVDNA was extracted and measured by qPCR. The data are represented as relative mean values to that of control siRNA (siControl)-treated cells with SEM of at least three independent experiments for each case (A, D, E, F, G, and H). Statistical analysis was done by one-way ANOVA with Dunnett's multiple comparisons test.

HBV replication is negatively regulated by the NMD pathway

Because a recent report suggested that both viral RNA and DNA replication are restricted by the NMD pathway,[19,22–24] we next tested whether NMD dysfunction by transfection with an siRNA targeting NMD factors would affect HBV replication in the natural life cycle. To uncover the contribution of the NMD pathway in HBV replication, we first checked the intracellular accumulation and encapsidation of pgRNA using HBV-inducible HepAD38.7 cells. NMD depletion resulted in significantly greater pgRNA/3.5 knt RNA accumulation compared to that in siControl-treated cells (Figure 5A). Similarly, we found that efficient accumulation of HBc protein was also observed in HBV-inducing cells with NMD depletion at early induction time (Figure 5B) but not at late induction time (Figure 3A). Northern blotting analysis also showed greater HBV-related mRNA expression in the NMD-depleted cells, including 2.4 and 2.1 knt RNA (Figure 5C). Accordingly, more HBeAg and HBsAg were detected in the soup in NMD-depleted cells (Figures 5D and 5E). Encapsidated pgRNA was also increased in the UPF1- and UPF2-depleted cells, though we did not observe a significant increase in the case of siSMG6 compared to the accumulated pgRNA (Figure 5F). Nevertheless, the levels of intracellular core-associated and extracellular particle-associated HBV DNA were clearly higher in the NMD-depleted cells (Figures 5G and 5H). Moreover, UPF1 depletion by short hairpin RNA also promoted HBV replication more efficiently (Figures S5A and S5B), while alternative rpL3 mRNA, which is not underregulated by Tet but rather by

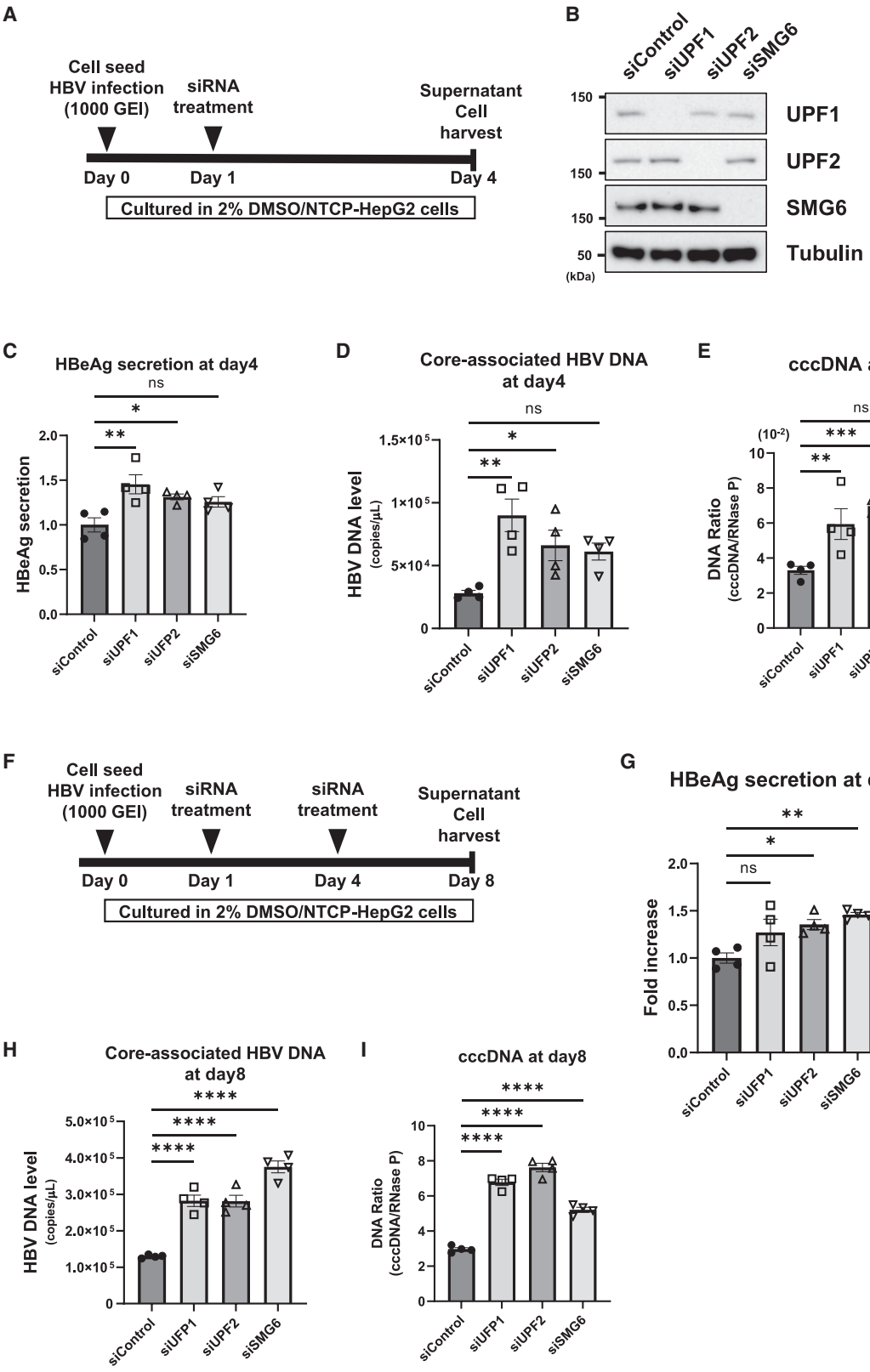

(legend on next page)

the NMD system, showed greater accumulation either with or without Tet compared to the canonical rpL3 mRNA (Figure S5C).

To exclude the possibility that the increased stability of HBV RNAs is caused by altered expression of host factors determining the fate of HBV RNA, we checked the protein expression levels of XRN1/2 as famous RNA executors, DDX17,[28] ZAP,[29] and RBM24[30] that are related to the stability of HBV RNAs, in NMD-depleted cells. Then, we did not find any altered expression of the host factors (Figure S6A). Additionally, we further checked whether HBV replication affected the protein expression of NMD-related factors. Using HBV replication plasmids encoding 1.25-fold genome, the protein levels of NMD-related factor were determined, and we did not observe any alteration of the expression (Figure S6B). Also, the expressions of NMD-related factors were not altered in HBV-inducible cells (Figure 3A). Indeed, NMD reporter assay also showed that HBV replication did not induce NMD suppression (Figure S6C). Thus, our data indicated no evidence that HBV replication directly or indirectly affected the NMD function and decay of HBV RNA.

Collectively, these data suggested that HBV gene expression and replication are restricted by the NMD pathway via its control of the stability of pgRNA/3.5 knt RNA and 2.4/2.1 knt RNA.

The NMD pathway restricts the early and late phases of the HBV infection cycle

Generally, the NMD pathway is a rapid RNA degradation process for aberrant transcripts in cytosol. Therefore, the recognition of viral RNAs by the NMD pathway should be critical during the HBV life cycle. To determine the NMD contribution to the HBV infection cycle, we inoculated HBV infectious particles into NMD-deficient human NTCP (sodium taurocholate co-transporting peptide)-expressing HepG2 cells (NTCP/G2), which are susceptible to HBV infection,[31] and checked the level of core-associated HBV DNA at 4 days post infection (Figure 6A). UPF1, UPF2, and SMG6 were consistently depleted by each siRNA in NTCP/G2 cells (Figure 6B). We found significant increases in secreted HBeAg and intracellular core-associated HBV DNA in UPF1- or UPF2-depleted cells compared to the levels in control cells, though siSMG6 had less effect again (Figures 6C and 6D).

Although depletion of SMG6 seemed not to affect the HBV life cycle significantly, secreted HBeAg and core-associated HBV DNA tended to increase when SMG6 was depleted (Figures 6C and 6D), indicating that SMG6 might make a little contribution to HBV replication (Figures 4C and 4E right). UPF1 or UPF2 depletion by short hairpin RNA also induced a similar effect—namely, HBV replication was promoted (Figures S7A–S7C).

Unexpectedly, we observed more cccDNA formation in HBV-infected cells that were depleted of UPF1 or UPF2 (Figure 6E), implying that these factors might affect molecules involved in the HBV attachment/entry process. Alternatively, it is not impossible that cccDNA formation was enhanced by pgRNA stabilization.

Because HBV is known as a pathogen showing lagged propagation in cell culture systems,[32] we further evaluated viral replication in the middle-late phase of virus propagation under NMD depletion (Figure 6F). At 8 days post infection, HBeAg secretion was increased in NMD-depleted cells, including siSMG6-treated cells (Figure 6G). In addition, we found that intracellular core-associated DNA was significantly increased in NMD-depleted cells (Figure 6H), and cccDNA formation was also increased at this phase in the cells (Figure 6I). These data suggest that the NMD pathway negatively controls the early and late phases of the HBV infection cycle as well.

DISCUSSION

Chronic HBV infection carries a high risk of lethal cirrhosis and HCC and has been recognized as one of the most serious world health problems. Even though HBV vaccination is an effective prophylaxis against infection, more than 260 million people are infected with HBV worldwide.[1] No reliable and highly effective antiviral therapies have yet been developed, largely because drug-resistant viruses frequently show up in patients with HBV and HBV cccDNA is very difficult to eradicate. To overcome these barriers and develop a novel HBV therapeutics, it is important to understand the interplay between targetable host factors and HBV infection/replication.

The NMD system was first shown to function in monitoring and quality control of viral RNAs in plant viruses.[24] It was later shown that the same system functions in mammalian viruses, not only RNA viruses such as alphavirus,[19] HCV,[20] ZIKV,[21] MHV,[22] and rotavirus[33] but also a DNA virus, KSHV.[23] Thus, therapies that

Figure 6. The NMD pathway governs HBV early replication in HBV-infected HepG2 cells

(A) Experimental protocol of HBV infection in human NTCP-expressing HepG2 (NTCP-HepG2) cells at the early phase of HBV infection.

(B) Protein levels in NMD-depleted NTCP-HepG2 cells infected with HBV (GEI at 1,000) at 4 days post infection (dpi).

(C) Level of secreted HBeAg at 4 dpi. HBeAg secreted into the culture medium at 4 dpi was measured with ELISA. The OD values were normalized by the amount of total protein, and data are shown as the fold excess relative to the value of the siControl group.

(D) Amount of intracellular HBV DNA (core-associated) at 4 dpi. Intracellular HBV DNA (core-associated) in HBV-infected cells at 4 dpi was prepared and measured by qPCR.

(E) The level of cccDNA in HBV-infected cells at 4 dpi. HBV cccDNA was prepared and measured by dPCR. The cellular RNase P copy number was also measured and used for normalization.

(F) Experimental protocol of the late stage of HBV infection.

(G) Levels of HBeAg secretion at 8 dpi. Secreted HBeAg at 8 dpi was measured with ELISA. OD values were normalized by the amount of total protein, and data are shown as the fold excess relative to the value of siControl group.

(H) Level of core-associated HBV DNA at 8 dpi. Core-associated HBV DNA was prepared and measured by qPCR.

(I) Level of cccDNA at 8 dpi. HBV cccDNA was prepared as described in the main text and measured by dPCR. The cellular RNase P copy number was also measured with dPCR and used for normalization.

All data are presented with the SEM of at least three independent experiments. Statistical analysis was done by one-way ANOVA with Dunnett's multiple comparisons test.

genetically or chemically affect the NMD pathway could be effective, because the NMD pathway is an intrinsic antiviral system against various infectious viruses.

The NMD pathway is a rapid RNA degradation system in the cytosol, and most foreign RNAs must face its surveillance. RNA surveillance systems such as non-stop decay (NSD) and non-go decay (NGD) are part of the machinery for control of cellular RNA quality and quantity against aberrant RNAs, including viral RNAs.[34] In this way, the RNA surveillance systems such as NMD, NSD, and NGD contribute to the control of various types of viral RNAs. For this reason, the NMD pathway has been a point of focus in the fields of virology and immunology as a means of cell-intrinsic immunity by targeting viral genomes and transcripts for the decay, although viruses tend to circumvent this system by using viral proteins or genomic sequences for efficient daughter virus production.[35]

The NMD system depends on *cis*-acting features such as long 3′ UTR and multiple ORFs in the transcripts, and these features subsequently attract various *trans*-acting protein factors to form mRNA-protein complexes, which execute the monitoring and quality control activities.[36] Mammal Stau1 is known as a key factor in Staufen-mediated mRNA decay; it is mediated by both UPF1 and UPF2 and binds to a specific structure of double-stranded RNA (dsRNA) in 3′ UTR.[37] In this study, we have revealed that virologically important HBV transcripts are targets of the NMD pathway, leading to the suppression of HBV gene expression and replication. Our data indicated that UPF1 and UPF2 were highly involved in HBV gene expression/replication through the stabilization of viral RNAs, but collaboration of Stau1 with UPF1 and UPF2 was unlikely, because HBV transcripts did not have any specific feature of dsRNA targeted by Stau1.

Interestingly, the first report on DNA virus suggested that the NMD pathway regulates reactivation of KSHV by controlling the expression levels of both host and viral transcripts exported to cytoplasm.[23] Consistent with this idea, our data also indicated that the stability of essential viral transcripts was regulated by core NMD factors via the regulation of viral replication. Thus, transcripts from not only RNA viruses but also DNA viruses are monitored by the NMD system to maintain the cellular environment, followed by restriction of viral replication and/or induction of innate immunity.

So far, it has not been reported whether the NMD surveillance system functions during the HBV life cycle. Unfortunately, we could not find any viral proteins that function as anti-NMD as reported in various viruses. In addition to that, HBV replication did not alter the expression of NMD-related factors and the function of the NMD pathway (Figures S6B and S6C). These suggest that HBV infection would not have molecular strategies against the NMD pathway. Interestingly, it has been suggested that pgRNA encapsidation initially occurs in the nucleus and very rarely in the cytosol, where HBV RNAs could be recognized by the NMD system.[38] Thus, it might be advantageous for HBV to undergo encapsidation in the nucleus to escape NMD surveillance. In the HBV infection system, cccDNA formation was increased in UPF1- and UPF2-depleted cells. It is thought that a level of cccDNA is coming from rcDNA entering into cells. NMD depletion was done after viral infection in our infection experiment, and thus, there is a possibility that pgRNA accumulation in the nucleus early phase of infection may promote formation of cccDNA as the internal cycle rather than genomic rcDNA synthesis as egress of daughter viruses.

Furthermore, our data indicated that NMD depletion highly enhanced pgRNA accumulation (∼7-fold in UPF1 depletion) but moderately increased encapsidated pgRNA (∼2.5-fold), leading to similar folds of HBV DNA formation in HBV-replicating cells (Figure 5). These data suggest that the increased amount of pgRNA does not strongly facilitate pgRNA encapsidation, while the NMD pathway just directly affects the stability of pgRNA. In addition to that, efficient accumulation of HBc protein was found in NMD-depleted cells at early induction time, and catch up the expression of HBc protein in NMD-depleted cells (Figures 3A and 5B). And, the first-round translated pgRNA will be recognized by the NMD pathway, probably, encapsidated pgRNA is not. In fact, we have shown in a decay assays of IVT-pgRNA that transfected pgRNA is not only used for encapsidation and translated into viral proteins but is also degraded by the NMD pathway (Figure 2A). These imply that the NMD pathway may regulate the fate of pgRNA followed by (1) conversion to cccDNA, (2) viral protein synthesis, and (3) pgRNA encapsidation during HBV replication.

Among HBV-related transcripts, X RNA seemed not to be a transcript targeted by the NMD machinery (Figure 2A right lower), because it is a typical mRNA that exclusively encodes X ORF with no long 3′ UTR. The HBx protein encoded by X RNA plays a key role in the development of HCC in the natural course of chronic HBV infection,[39,40] and thus, there is a possibility that X becomes more competent for hepatocarcinogenesis by escaping the NMD system. On the other hand, there is a report describing that the NSD pathway mediates the decay of X RNA by recruiting RNA exosomes.[41]

The NMD pathway globally inspects and controls the quality of intracellular mRNA. This includes not only major viral transcripts but also alternative viral transcripts during HBV infection; e.g., minor spliced pgRNAs[42–44] may be targets. Interestingly, our data indicated that UPF2, one of EJC proteins attached after host splicing, has an impact on HBV replication as well as UPF1, implying that spliced HBV transcripts could be likely a target of the NMD pathway. In addition, several HBV spliced proteins (HBVSPs) translated from spliced pgRNA or 3.5 knt RNA suppressed the transduction of interferon alpha (IFN-α) signaling, resulting in HBV resistance to IFN-mediated host defenses.[45] Thus, there is a possibility that the enhancement of HBV replication by NMD depletion may be due in part to the accumulation of spliced pgRNA encoding specific HBVSPs to suppress the IFN response.

Taken together, our findings suggest that major HBV transcripts (pgRNA/3.5 knt RNA, 2.4/2.1 knt RNA) are subject to NMD monitoring to maintain the cellular environment and that such monitoring constitutes a cell-intrinsic antiviral system against HBV infection. The insights from this study are expected to inform research into other DNA virus life cycles, and the accumulating evidence from such efforts will clarify the roles of the NMD pathway against various viruses and ultimately provide clues toward the development of antivirals.

Limitations of the study

In this study, we found that the NMD pathway, a host mechanism, is a mechanism for controlling HBV RNA expression in hepatic cell lines. However, HBV RNA that escapes surveillance continues to replicate and forms cccDNA, which does not lead to complete HBV treatment. Another limitation is a technology has not yet been established to control NMD function; thus, further development of research is required.

RESOURCE AVAILABILITY

Lead contact

Further information and requests for resources and reagents should be directed to and will be fulfilled by the lead contact, Masami Wada (mawada@virus.med.osaka-u.ac.jp).

Materials availability

All materials used in this study are available from the lead contact with a completed material transfer agreement. This study did not generate new unique reagents.

Data and code availability

- All data reported in this paper will be shared by the lead contact upon request.
- This paper does not report original code.

ACKNOWLEDGMENTS

The authors gratefully acknowledge Ms. H. Otake and Ms. Hashimoto for their invaluable technical assistance with the experiments and Dr. Kurosaki and Dr. Maquat, University of Rochester, MN, for providing the NMD reporter plasmids. This research was supported by a JSPS Grant-in-Aid for Young Scientists (no. JP-19K166680) to M.W. and by Japan Agency for Medical Research and Development (AMED) Grants (nos. 16fk0310504h0005, 17fk0310105h0001, 18fk0310105h0002, 19fk0310105h0003, 20fk0310105h0004, 21fk310105h005, 22fk0310505h0001, and 23fk0310505h0002) to K.U.

AUTHOR CONTRIBUTIONS

Study conception and design, M.W., C.M., E.O., and K.U.; acquisition of data, M.W.; analysis and interpretation of data, M.W. and K.U.; drafting of manuscript, M.W. and K.U.

DECLARATION OF INTERESTS

The authors declare no competing interests.

STAR★METHODS

Detailed methods are provided in the online version of this paper and include the following:

SUPPLEMENTAL INFORMATION

Supplemental information can be found online at https://doi.org/10.1016/j.isci.2025.112460.

Received: July 25, 2024
Revised: November 28, 2024
Accepted: April 11, 2025
Published: April 16, 2025

REFERENCES

1. Trépo, C., Chan, H.L.Y., and Lok, A. (2014). Hepatitis B virus infection. Lancet *384*, 2053–2063. https://doi.org/10.1016/s0140-6736(14)60220-8.
2. Jeng, W.J., Papatheodoridis, G.V., and Lok, A.S.F. (2023). Hepatitis B. Lancet *401*, 1039–1052. https://doi.org/10.1016/s0140-6736(22)01468-4.
3. Michel, M.L., and Tiollais, P. (1987). Structure and expression of the hepatitis B virus genome. Hepatology *7*, 61s–63s. https://doi.org/10.1002/hep.1840070711.
4. Seeger, C., and Mason, W.S. (2015). Molecular biology of hepatitis B virus infection. Virology *479–480*, 672–686. https://doi.org/10.1016/j.virol.2015.02.031.
5. Ablasser, A., and Hur, S. (2020). Regulation of cGAS- and RLR-mediated immunity to nucleic acids. Nat. Immunol. *21*, 17–29. https://doi.org/10.1038/s41590-019-0556-1.
6. Hu, M.M., and Shu, H.B. (2018). Cytoplasmic Mechanisms of Recognition and Defense of Microbial Nucleic Acids. Annu. Rev. Cell Dev. Biol. *34*, 357–379. https://doi.org/10.1146/annurev-cellbio-100617-062903.
7. Cai, X., Zhou, Z., Zhu, J., Liu, X., Ouyang, G., Wang, J., Li, Z., Li, X., Zha, H., Zhu, C., et al. (2022). Opposing effects of deubiquitinase OTUD3 in innate immunity against RNA and DNA viruses. Cell Rep. *39*, 110920. https://doi.org/10.1016/j.celrep.2022.110920.
8. Brisse, M., and Ly, H. (2019). Comparative Structure and Function Analysis of the RIG-I-Like Receptors: RIG-I and MDA5. Front. Immunol. *10*, 1586. https://doi.org/10.3389/fimmu.2019.01586.
9. Yang, G., Wan, P., Zhang, Y., Tan, Q., Qudus, M.S., Yue, Z., Luo, W., Zhang, W., Ouyang, J., Li, Y., and Wu, J. (2022). Innate Immunity, Inflammation, and Intervention in HBV Infection. Viruses *14*, 2275. https://doi.org/10.3390/v14102275.
10. Megahed, F.A.K., Zhou, X., and Sun, P. (2020). The Interactions between HBV and the Innate Immunity of Hepatocytes. Viruses *12*, 285. https://doi.org/10.3390/v12030285.
11. Schweingruber, C., Rufener, S.C., Zünd, D., Yamashita, A., and Mühlemann, O. (2013). Nonsense-mediated mRNA decay - mechanisms of substrate mRNA recognition and degradation in mammalian cells. Biochim. Biophys. Acta *1829*, 612–623. https://doi.org/10.1016/j.bbagrm.2013.02.005.
12. Isken, O., Kim, Y.K., Hosoda, N., Mayeur, G.L., Hershey, J.W.B., and Maquat, L.E. (2008). Upf1 phosphorylation triggers translational repression during nonsense-mediated mRNA decay. Cell *133*, 314–327. https://doi.org/10.1016/j.cell.2008.02.030.
13. Maquat, L.E., Tarn, W.Y., and Isken, O. (2010). The pioneer round of translation: features and functions. Cell *142*, 368–374. https://doi.org/10.1016/j.cell.2010.07.022.

14. Durand, S., and Lykke-Andersen, J. (2013). Nonsense-mediated mRNA decay occurs during eIF4F-dependent translation in human cells. Nat. Struct. Mol. Biol. *20*, 702–709. https://doi.org/10.1038/nsmb.2575.

15. Le Hir, H., Gatfield, D., Braun, I.C., Forler, D., and Izaurralde, E. (2001). The protein Mago provides a link between splicing and mRNA localization. EMBO Rep. *2*, 1119–1124. https://doi.org/10.1093/embo-reports/kve245.

16. Lykke-Andersen, J., Shu, M.D., and Steitz, J.A. (2001). Communication of the position of exon-exon junctions to the mRNA surveillance machinery by the protein RNPS1. Science *293*, 1836–1839. https://doi.org/10.1126/science.1062786.

17. Yamashita, A., Ohnishi, T., Kashima, I., Taya, Y., and Ohno, S. (2001). Human SMG-1, a novel phosphatidylinositol 3-kinase-related protein kinase, associates with components of the mRNA surveillance complex and is involved in the regulation of nonsense-mediated mRNA decay. Genes Dev. *15*, 2215–2228. https://doi.org/10.1101/gad.913001.

18. Mendell, J.T., Sharifi, N.A., Meyers, J.L., Martinez-Murillo, F., and Dietz, H. C. (2004). Nonsense surveillance regulates expression of diverse classes of mammalian transcripts and mutes genomic noise. Nat. Genet. *36*, 1073–1078. https://doi.org/10.1038/ng1429.

19. Balistreri, G., Horvath, P., Schweingruber, C., Zünd, D., McInerney, G., Merits, A., Mühlemann, O., Azzalin, C., and Helenius, A. (2014). The host nonsense-mediated mRNA decay pathway restricts Mammalian RNA virus replication. Cell Host Microbe *16*, 403–411. https://doi.org/10.1016/j.chom.2014.08.007.

20. Ramage, H.R., Kumar, G.R., Verschueren, E., Johnson, J.R., Von Dollen, J., Johnson, T., Newton, B., Shah, P., Horner, J., Krogan, N.J., and Ott, M. (2015). A combined proteomics/genomics approach links hepatitis C virus infection with nonsense-mediated mRNA decay. Mol. Cell *57*, 329–340. https://doi.org/10.1016/j.molcel.2014.12.028.

21. Fontaine, K.A., Leon, K.E., Khalid, M.M., Tomar, S., Jimenez-Morales, D., Dunlap, M., Kaye, J.A., Shah, P.S., Finkbeiner, S., Krogan, N.J., and Ott, M. (2018). The Cellular NMD Pathway Restricts Zika Virus Infection and Is Targeted by the Viral Capsid Protein. mBio *9*, e02126-18. https://doi.org/10.1128/mBio.02126-18.

22. Wada, M., Lokugamage, K.G., Nakagawa, K., Narayanan, K., and Makino, S. (2018). Interplay between coronavirus, a cytoplasmic RNA virus, and nonsense-mediated mRNA decay pathway. Proc. Natl. Acad. Sci. USA *115*, E10157–E10166. https://doi.org/10.1073/pnas.1811675115.

23. Zhao, Y., Ye, X., Shehata, M., Dunker, W., Xie, Z., and Karijolich, J. (2020). The RNA quality control pathway nonsense-mediated mRNA decay targets cellular and viral RNAs to restrict KSHV. Nat. Commun. *11*, 3345. https://doi.org/10.1038/s41467-020-17151-2.

24. Garcia, D., Garcia, S., and Voinnet, O. (2014). Nonsense-mediated decay serves as a general viral restriction mechanism in plants. Cell Host Microbe *16*, 391–402. https://doi.org/10.1016/j.chom.2014.08.001.

25. May, J.P., Yuan, X., Sawicki, E., and Simon, A.E. (2018). RNA virus evasion of nonsense-mediated decay. PLoS Pathog. *14*, e1007459. https://doi.org/10.1371/journal.ppat.1007459.

26. Cuccurese, M., Russo, G., Russo, A., and Pietropaolo, C. (2005). Alternative splicing and nonsense-mediated mRNA decay regulate mammalian ribosomal gene expression. Nucleic Acids Res. *33*, 5965–5977. https://doi.org/10.1093/nar/gki905.

27. Ladner, S.K., Otto, M.J., Barker, C.S., Zaifert, K., Wang, G.H., Guo, J.T., Seeger, C., and King, R.W. (1997). Inducible expression of human hepatitis B virus (HBV) in stably transfected hepatoblastoma cells: a novel system for screening potential inhibitors of HBV replication. Antimicrob. Agents Chemother. *41*, 1715–1720. https://doi.org/10.1128/aac.41.8.1715.

28. Mao, R., Dong, M., Shen, Z., Zhang, H., Liu, Y., Cai, D., Mitra, B., Zhang, J., and Guo, H. (2021). RNA Helicase DDX17 Inhibits Hepatitis B Virus Replication by Blocking Viral Pregenomic RNA Encapsidation. J. Virol. *95*, e0044421. https://doi.org/10.1128/jvi.00444-21.

29. Mao, R., Nie, H., Cai, D., Zhang, J., Liu, H., Yan, R., Cuconati, A., Block, T. M., Guo, J.T., and Guo, H. (2013). Inhibition of hepatitis B virus replication by the host zinc finger antiviral protein. PLoS Pathog. *9*, e1003494. https://doi.org/10.1371/journal.ppat.1003494.

30. Yao, Y., Yang, B., Cao, H., Zhao, K., Yuan, Y., Chen, Y., Zhang, Z., Wang, Y., Pei, R., Chen, J., et al. (2018). RBM24 stabilizes hepatitis B virus pregenomic RNA but inhibits core protein translation by targeting the terminal redundancy sequence. Emerg. Microbes Infect. *7*, 86. https://doi.org/10.1038/s41426-018-0091-4.

31. Iwamoto, M., Watashi, K., Tsukuda, S., Aly, H.H., Fukasawa, M., Fujimoto, A., Suzuki, R., Aizaki, H., Ito, T., Koiwai, O., et al. (2014). Evaluation and identification of hepatitis B virus entry inhibitors using HepG2 cells overexpressing a membrane transporter NTCP. Biochem. Biophys. Res. Commun. *443*, 808–813. https://doi.org/10.1016/j.bbrc.2013.12.052.

32. Xiang, C., Du, Y., Meng, G., Soon Yi, L., Sun, S., Song, N., Zhang, X., Xiao, Y., Wang, J., Yi, Z., et al. (2019). Long-term functional maintenance of primary human hepatocytes *in vitro*. Science *364*, 399–402. https://doi.org/10.1126/science.aau7307.

33. Sarkar, R., Banerjee, S., Mukherjee, A., and Chawla-Sarkar, M. (2022). Rotaviral nonstructural protein 5 (NSP5) promotes proteasomal degradation of up-frameshift protein 1 (UPF1), a principal mediator of nonsense-mediated mRNA decay (NMD) pathway, to facilitate infection. Cell. Signal. *89*, 110180. https://doi.org/10.1016/j.cellsig.2021.110180.

34. Morris, C., Cluet, D., and Ricci, E.P. (2021). Ribosome dynamics and mRNA turnover, a complex relationship under constant cellular scrutiny. Wiley Interdiscip. Rev. RNA *12*, e1658. https://doi.org/10.1002/wrna.1658.

35. Mocquet, V., Neusiedler, J., Rende, F., Cluet, D., Robin, J.P., Terme, J.M., Duc Dodon, M., Wittmann, J., Morris, C., Le Hir, H., et al. (2012). The human T-lymphotropic virus type 1 tax protein inhibits nonsense-mediated mRNA decay by interacting with INT6/EIF3E and UPF1. J. Virol. *86*, 7530–7543. https://doi.org/10.1128/jvi.07021-11.

36. Carrard, J., and Lejeune, F. (2023). Nonsense-mediated mRNA decay, a simplified view of a complex mechanism. BMB Rep. *56*, 625–632. https://doi.org/10.5483/BMBRep.2023-0190.

37. Gowravaram, M., Schwarz, J., Khilji, S.K., Urlaub, H., and Chakrabarti, S. (2019). Insights into the assembly and architecture of a Staufen-mediated mRNA decay (SMD)-competent mRNP. Nat. Commun. *10*, 5054. https://doi.org/10.1038/s41467-019-13080-x.

38. Yang, C.C., Chang, C.H., Chen, H.L., Chou, M.C., Yang, C.J., Jhou, R.S., Huang, E.Y., Li, H.C., Suen, C.S., Hwang, M.J., and Shih, C. (2022). CRM1-spike-mediated nuclear export of hepatitis B virus encapsidated viral RNA. Cell Rep. *38*, 110472. https://doi.org/10.1016/j.celrep.2022.110472.

39. Wang, F., Song, H., Xu, F., Xu, J., Wang, L., Yang, F., Zhu, Y., and Tan, G. (2023). Role of hepatitis B virus non-structural protein HBx on HBV replication, interferon signaling, and hepatocarcinogenesis. Front. Microbiol. *14*, 1322892. https://doi.org/10.3389/fmicb.2023.1322892.

40. Papatheodoridi, A., and Papatheodoridis, G. (2023). Hepatocellular carcinoma: The virus or the liver? Liver Int. *43*, 22–30. https://doi.org/10.1111/liv.15253.

41. Aly, H.H., Suzuki, J., Watashi, K., Chayama, K., Hoshino, S.I., Hijikata, M., Kato, T., and Wakita, T. (2016). RNA Exosome Complex Regulates Stability of the Hepatitis B Virus X-mRNA Transcript in a Non-stop-mediated (NSD) RNA Quality Control Mechanism. J. Biol. Chem. *291*, 15958–15974. https://doi.org/10.1074/jbc.M116.724641.

42. Ito, N., Nakashima, K., Sun, S., Ito, M., and Suzuki, T. (2019). Cell Type Diversity in Hepatitis B Virus RNA Splicing and Its Regulation. Front. Microbiol. *10*, 207. https://doi.org/10.3389/fmicb.2019.00207.

43. Kremsdorf, D., Lekbaby, B., Bablon, P., Sotty, J., Augustin, J., Schnuriger, A., Pol, J., and Soussan, P. (2021). Alternative splicing of viral transcripts: the dark side of HBV. Gut *70*, 2373–2382. https://doi.org/10.1136/gutjnl-2021-324554.

44. Wang, Y.L., Liou, G.G., Lin, C.H., Chen, M.L., Kuo, T.M., Tsai, K.N., Huang, C.C., Chen, Y.L., Huang, L.R., Chou, Y.C., and Chang, C. (2015). The

inhibitory effect of the hepatitis B virus singly-spliced RNA-encoded p21.5 protein on HBV nucleocapsid formation. PLoS One *10*, e0119625. https://doi.org/10.1371/journal.pone.0119625.

45. Chen, J., Wu, M., Wang, F., Zhang, W., Wang, W., Zhang, X., Zhang, J., Liu, Y., Liu, Y., Feng, Y., et al. (2015). Hepatitis B virus spliced variants are associated with an impaired response to interferon therapy. Sci. Rep. *5*, 16459. https://doi.org/10.1038/srep16459.

46. Fauzyah, Y., Ono, C., Torii, S., Anzai, I., Suzuki, R., Izumi, T., Morioka, Y., Maeda, Y., Okamoto, T., Fukuhara, T., and Matsuura, Y. (2021). Ponesimod suppresses hepatitis B virus infection by inhibiting endosome maturation. Antiviral Res. *186*, 104999. https://doi.org/10.1016/j.antiviral.2020.104999.

47. Sugiyama, M., Tanaka, Y., Kato, T., Orito, E., Ito, K., Acharya, S.K., Gish, R.G., Kramvis, A., Shimada, T., Izumi, N., et al. (2006). Influence of hepatitis B virus genotypes on the intra- and extracellular expression of viral DNA and antigens. Hepatology *44*, 915–924. https://doi.org/10.1002/hep.21345.

48. Nakayama, R., Ueno, Y., Ueda, K., and Honda, T. (2019). Latent infection with Kaposi's sarcoma-associated herpesvirus enhances retrotransposition of long interspersed element-1. Oncogene *38*, 4340–4351. https://doi.org/10.1038/s41388-019-0726-5.

49. Kurosaki, T., Li, W., Hoque, M., Popp, M.W.L., Ermolenko, D.N., Tian, B., and Maquat, L.E. (2014). A post-translational regulatory switch on UPF1 controls targeted mRNA degradation. Genes Dev. *28*, 1900–1916. https://doi.org/10.1101/gad.245506.114.

50. Zhang, J., Sun, X., Qian, Y., and Maquat, L.E. (1998). Intron function in the nonsense-mediated decay of beta-globin mRNA: indications that pre-mRNA splicing in the nucleus can influence mRNA translation in the cytoplasm. RNA *4*, 801–815. https://doi.org/10.1017/s1355838298971849.

51. Liu, X.Q., Ohsaki, E., and Ueda, K. (2020). Establishment of a system for finding inhibitors of ε RNA binding with the HBV polymerase. Genes Cells *25*, 523–537. https://doi.org/10.1111/gtc.12778.

52. Muriungi, N.G., and Ueda, K. (2020). TIMM29 interacts with hepatitis B virus preS1 to modulate the HBV life cycle. Microbiol. Immunol. *64*, 792–809. https://doi.org/10.1111/1348-0421.12852.

STAR★METHODS

KEY RESOURCES TABLE

REAGENT or RESOURCE	SOURCE	IDENTIFIER
Antibodies		
Rabbit anti-UPF1 antibody	Cell Signaling Technology	Cat#9435; RRID: AB_10629662
Mouse anti-RENT2/UPF2 antibody	Santa Cruz Bio. Inc.	Cat#sc-374230; RRID: AB_10988267
Rabbit anti-SMG6 antibody	Abcam	Cat#ab87539; RRID: AB_10674461
Rabbit anti-phosphorylated UPF1 (Ser1127)	Millipore	Cat#07-1016; RRID: AB_10805931
Mouse anti-HBs antibody	Beacle Inc.	Cat#BCL-ABMS-02
Mouse anti-HBV PreS1 antibody	Beacle Inc.	Cat#BCL-ABM1-02
Mouse anti-HBV PreS2 antibody	Beacle Inc.	Cat#BCL-ABM2-02
Rabbit anti-HBc antibody	Beacle Inc.	Cat#BCL-ABPC-01
Rabbit anti-XRN1 antibody	Cell Signaling Technology	Cat#70205; RRID: AB_2799779
Rabbit anti-XRN2 antibody	Cell Signaling Technology	Cat#13760; RRID: AB_2798309
Rabbit anti-ZAP antibody	Cell Signaling Technology	Cat#33750
Mouse anti-DDX17 antibody	Proteintech.	Cat#19910-1-AP; RRID: AB_10667004
Rabbit anti-RBM24 antibody	Abcam	Cat#ab94567; RRID: AB_10674832
Mouse anti-GFP antibody	Nacalai Tesque	Cat#04363-24; RRID: AB_3675836
Mouse anti-βTubulin antibody	Sigma Aldrich	Cat#T5201; RRID: AB_609915
Anti-mouse IgG HRP conjugated	Dako	Cat#P0447; RRID: AB_2617137
Anti-rabbit IgG HRP conjugated	Dako	Cat#P0448; RRID: AB_2617138
Rabbit immunoglobulin Fraction (normal)	Dako	Cat#X0903; RRID: AB_906174
Anti-mouse IgG conjugated with Alexa® 488	Thermo Fisher Scientific	Cat#A-11001; RRID: AB_2534069
Anti-rabbit IgG conjugated with Alexa® 546	Thermo Fisher Scientific	Cat#A-11035; RRID: AB_143051
Bacterial and virus strains		
pLKO.1 puro lentivirus	Addgene	Cat#8453
Recombinant HBV, genotype D	Ladner et al.[27]	N/A
pHBV WT, HBV genotype C (#AB246345.1)	Fauzyah et al.[46] Sugiyama et al.[47]	N/A
pHBV pol dead	This paper	N/A
Chemicals, peptides, and recombinant proteins		
Cycloheximide	Sigma Aldrich	Cat# 239763
Wortmannin	Sigma Aldrich	Cat# 681675
Okadaic acid	FUJIFILM	Cat#152-03271
Hydrocortisone	Sigma Aldrich	Cat#H0396
Human insulin	Sigma Aldrich	Cat#I9278
EGF Recombinant Human Protein	Thermo Fisher Scientific	Cat#PHG0313
Sodium Selenite	Sigma Aldrich	Cat#S9133
Transferin (Holo) from Human blood	FUJIFILM	Cat#208-18971
Recombinat DNase I, RNase free	TaKaRa	Cat#2270A
Recombinant RNase inhibitor	TaKaRa	Cat#2313A
Dynabeads™ Protein G-conjugated	Thermo Fisher Scientific	Cat#10004D
TRIzol™ LS reagent	Thermo Fisher Scientific	Cat#10296028
TRIzol™ reagent	Thermo Fisher Scientific	Cat#15596018
Critical commercial assays		
HBeAg Diagnostic kit	Shanghai RSbio	N/A
HB S antigen quantitative ELISA kit Rapid-II	Beacle Inc	Cat#BCL-SHP-21

(*Continued on next page*)

Continued

REAGENT or RESOURCE	SOURCE	IDENTIFIER
HBs PreS-1 antigen quantitative ELISA kit Rapid	Beacle Inc	Cat#BCL-S1HP-01
HBs PreS-2 antigen quantitative ELISA kit Rapid	Beacle Inc	Cat#BCL-S2HP-01
mMESSAGE mMACHINE™ T7 transcription kit	Thermo Fisher Scientific	Cat#AM1344
AmpliCap-Max T7 High Yield Message Maker Kit	CellScript	Cat#C-ACM04037
A-Plus Poly(A) Polymerase Tailing Kit	CellScript	Cat#C-PAP5104H
Maxwell® RSC genomic DNA kit	Promega	Cat#AS1880
Direct-zol RNA Miniprep Kit	Zymo Research	Cat#R2052
DIG RNA labeling kit (SP6/T7)	Roche	Cat#11175025910
GenJetTM *In Vitro* DNA Transfection Reagent for HepG2 Cells	SignaGen Laboratories	Cat#SL100489-HEPG2
Absolute Q™ DNA Digital PCR Master Mix	Thermo Fisher Scientific	Cat#A52490
Experimental models: Cell lines		
Human: NTCP-expressing HepG2 cells	Iwamoto et al.[31]	N/A
Human: HepAD38.7 cells	Ladner et al.[27]	N/A
Human: LentiX HEK293T cells	Clontech	Cat# 632180
Oligonucleotides		
siRNA targeting sequence (see Table S1)	This paper	N/A
shRNA targeting sequence (see Table S1)	This paper	N/A
Primers for plasmid cloning (see Table S1)	This paper	N/A
Primers for qPCR and dPCR (see Table S1)	This paper	N/A
Recombinant DNA		
pcDNA3.1	Thermo Fisher Scientific	Cat#V79020
pT7-pgRNA	This paper	N/A
pT7-pgRNA poldead	This paper	N/A
pT7-2.4kb RNA	This paper	N/A
pT7-2.1kb RNA	This paper	N/A
pT7-Small S RNA	This paper	N/A
pT7-XRNA	This paper	N/A
pRL-TK	Promega	Cat#E2241
pcDNA-GFP	Nakayama et al.[48]	N/A
pHBV-WT	Fauzyah et al.[46] Sugiyama et al.[47]	N/A
pHBV pol dead	This paper	N/A
pSPT18	Roche	Cat#11175025910
pSPT18-HBVRNA	This paper	N/A
pSPT18-hGAPDH	This paper	N/A
pCMV-globin Norm	Kurosaki et al.[49]; Zhang et al.[50]	N/A
pCMV-globin Ter39	Kurosaki et al.[49]; Zhang et al.[50]	N/A
pCMV-mMUP	This paper	N/A
pLKO-shUPF1	This paper	N/A
pLKO-shUPF2	This paper	N/A
pLKO puro	Addgene	Cat#8453
Software and algorithms		
GraphPad Prism9	GraphPad	N/A

EXPERIMENTAL MODEL AND STUDY PARTICIPANT DETAILS

Cell culture

Human sodium taurocholate co-transporting polypeptide (NTCP)-expressing HepG2 cells (NTCP/G2)[31] were grown in William's E medium (Gibco) supplemented with 10% fetal bovine serum (FBS) (Sigma-Aldrich), 1% antibiotic-antimycotic solution (100 units/mL penicillin, 100 μg/mL streptomycin, 0.25 μg/mL amphotericin B; Nacalai Tesque), 2 mM L-glutamine (Nacalai Tesque), 50 μM hydrocortisone (Sigma-Aldrich), 5 μg/ml insulin (Sigma-Aldrich), 10 ng/ml EGF (Thermo Fisher Scientific), 5 μg/mL holo-transferrin (Wako), 5 ng/ml sodium selenite (Sigma-Aldrich) (primary hepatocyte maintain media: PMM), and 0.5 mg/ml G418 (Nacalai Tesque).

HepAD38.7 cells[27] were cultured in DMEM/F12 (Nacalai Tesque) supplemented with 10% FBS, 1% antibiotic-antimycotic solution as above, 0.5 mg/ml G418, 5 μg/ml human insulin and 400 ng/ml tetracycline (Tet) (Nacalai Tesque).

HEK293T cells used for *in vitro* transcribed viral RNA transfection and lentivirus production, were grown in high glucose DMEM (Nacalai Tesque) supplemented with 10% FBS and the antibiotics as above. All cells were cultured at 37°C and 5% CO_2.

Viruses

To prepare HBV inoculum for the infection experiment, HepAD38.7 cells were cultured in the Tet-free culture medium and the cultured medium was accumulated every 5 days for 2 weeks. The medium was precipitated with a final concentration of 6% PEG8000, resuspended in PBS and concentrated. The virus titer was measured with quantitative PCR (qPCR) (see below).

Lentiviruses for NMD knockdown were produced by transfection with pLKO-control (shControl-sense/shControl-antisense), pLkO-UPF1 (human shUpf1-sense1/human shUpf1-antisense1) or -UPF2 (human shUpf2-sense/human shUpf2-antisense) using Lenti-X™ Packaging Single Shots (VSV-G) (Takara Bio Clontech) into HEK293T cells according to the manufacturer's protocol. At 3 days post-transfection, the culture medium containing recombinant lentiviruses was collected. Subsequently, HBV-infected NTCP-HepG2 cells were infected with these inoculums for NMD knockdown at 12 hrs before HBV infection. Short hairpin RNA sequences are described in the Table S1.

METHOD DETAILS

Plasmids

For construction of each plasmid driven by a T7 promoter coding viral transcript including pol-dead pgRNA, pcDNA3.1 was linearized by NruI and EcoRI. The HBV pgRNA/3.5 knt RNA region was amplified with two primer sets (pgRNAT7-infu-Fw and pgRNAmid-infu-Rv for fragment 1, and pgRNAmid-infu-Fw and HBV mRNA-infu-Rv for fragment 2). The amplified fragments were tandemly inserted into the linearized pcDNA3.1 by an In-Fusion® system (Takara Bio Inc.). The HBV pgRNA pol dead region was amplified with pgRNAT7-infu-Fw and pgRNApol dead-mid-infu-Rv for fragment 1, and pgRNApol dead-mid-infu-Fw and HBVmRNA-infu-Rv for fragment 2. The amplified fragments were tandemly inserted into the linearized pcDNA3.1 by an In-Fusion® system. Then, the HBV 2.1 knt RNA region was amplified with 2.1kb T7-infu-Fw and HBVmRNA-infu-Rv, and the non-authentic Small S RNA region was amplified with SmallST7-infu-Fw and HBVmRNA-infu-Rv. Each amplified fragment was inserted into the linearized pcDNA3.1 by an In-Fusion® system. The HBV 2.4 knt RNA region was amplified with 2.4kbT7-NruI-Fw and HBV RNA-EcoRI-Rv, and the HBV X RNA region was amplified with X mRNAT7-NruI-Fw and HBV RNA-EcoRI-Rv, respectively. The primer sequences are shown in Table S1. The amplified fragments were digested by NruI and EcoRI followed by insertion into the NruI and EcoRI sites of pcDNA3.1 with ligation high™ Ver2 (TOYOBO). pHB I-WT (adr4, genotype C) used as an amplification template contains 1.5 HBV genome (adr4, genotype C; GenBank: # LC090200.1) from the BamHI site at 1400nt-(3.2kb)-1400nt-BglII site at 1984nt. pcDNA3-GFP was the kind gift of Dr. Honda at Okayama University,[48] and pRL-TK was purchased from Promega.

An HBV replication plasmid (pHBV-WT) (GenBank: #AB246345.1) were provided from Dr. Ono and Dr. Matsuura,[46,47] and pHBV-pol dead was constructed by a point mutation (Threonine to stop codon at 163 aa in the POL ORF) introduced into pol of pHBV WT by mutagenesis. Briefly, pHBV pol-WT sequences were amplified using a set of primers (pHBV-pol dead-Fw and pHBV pol dead-Rv) and, then liner pHBV fragment harboring mutation on POL ORF was synthesized. This PCR product was treated with DpnI to remove template plasmids, and then treated with T4 Polynucleotide Kinase (Takara) to add a γ-phosphate group of ATP to the 5' end of this fragment for the self-ligation.

Lentiviral knockdown plasmid (pLKO1.puro; Addgene) was constructed by insertion of a dsDNA oligo that encodes a short hairpin for silencing *UPF1* (human shUpf1-sense1/ human shUpf1-antisense1) or *UPF2* (human shUpf2-sense/ human shUpf2-antisense). The NMD reporter plasmids, pCMV®-globin Norm and Ter39, were the kind gift of Dr. Maquat,[49,50] and an internal control plasmid, pCMV mMUP, was constructed by replacement of the *globin* gene in pCMV®-globin Norm with the mouse *MUP* gene using an In-Fusion® system at NcoI-NdeI sites. Mouse MUP ORF was amplified by PCR.

Plasmids for RNA probe synthesis were constructed by insertion of PCR product using pSPT18 linearized by XbaI and EcoRI. The PCR products were amplified with pSPT18-HBVRNA-XbaIFw and pSPT18-HBVRNA-EcoRIRv for HBV RNA probe and pSPT18-hGAPDH-infuF and pSPT18-hGAPDH-infuR for hGAPDH mRNA probe. The amplified fragment of HBV RNA was digested by XbaI and EcoRI followed by insertion into the XbaI and EcoRI sites of pSPT18 with ligation high™ Ver2 (TOYOBO). The amplified fragment of hGAPDH was inserted into the linearized pSPT18 by an In-Fusion® system.

All primer sets and dsDNAs are listed in Table S1.

In vitro transcription of HBV RNA

Capped and polyadenylated viral RNAs (pgRNA, pgRNA pol dead, 2.4 knt, 2.1 knt, Small S and X RNA) were produced *in vitro* from T7 promoter-driven plasmids, which were pcDNA 3.1 constructs containing the respective region, using an AmpliCap-Max T7 High Yield Message Maker Kit (CellScript) or mMESSEGE mMACHINE™ T7 transcription kit (Thermo Fisher Scientific) and a Plus Poly (A) Polymerase Tailing Kit (CellScript) according to the manufacturer's protocol. GPF mRNA and Renilla luciferase (rLuc) mRNA were also generated from T7 promoter-driven plasmids (pcDNA3-GFP and pRL-TK, respectively).

Small interfering RNA (siRNA) treatment

Double-stranded siRNAs listed in Table S1 (human UPF1,2 SMG6 and the control [siControl]) were synthesized and annealed by a manufacturer (FASMAC).

HEK293T cells were treated with each siRNA for the NMD factor (UPF1, UPF2 and SMG6) at 25 nM with Lipofectamine RNAiMAX (Thermo Fisher Scientific) according to the manufacturer's protocol for degradation kinetics assay.

HepAD38.7 cells cultured in the Tet-containing medium described above were split and incubated in antibiotics-free medium to induce HBV replication before siRNA transfection. At 12 hours (hrs) post-Tet removal, the cells were transfected with each siRNA for the NMD factor (UPF1, UPF2 and SMG6) at 25 nM with Lipofectamine RNAiMAX (Thermo Fisher Scientific) according to the manufacturer's protocol for degradation kinetics assay.

Assay of degradation kinetics of HBV transcripts in HEK293T cells

Purified IVTs were directly transfected into siRNA-mediated knocked down 293T cells using Lipofectamine MessengerMAX (Thermo Fisher Scientific). After 1 hr absorption of IVTs, the cells were twice rinsed with fresh complete media without antibiotics to wash out excess IVTs, and then the medium was replaced with fresh medium without antibiotics and the cells were incubated until the indicated time point. Then the cells were lysed with TRIzol® reagent (Thermo Fisher Scientific) for purification of total RNA, which was subjected to RT-qPCR (see below).

Assay of degradation kinetics of pgRNA/3.5 knt RNA in HepAD38.7 cells

NMD factor-depleted HepAD38.7 cells were further incubated for 36 hrs or 60 hrs without Tet. Then, the cells were re-treated with Tet to inhibit viral transcription for 8 hrs. The cells were lysed with TRIzol® reagent (Thermo Fisher Scientific) for purification of total RNA, followed by RT-qPCR or Northern blotting analysis (see below). Also, the stability of HBV pgRNA/3.5 knt RNA was evaluated in the presence of actinomycin D (ActD) and NMD inhibitors in HBV-induced HepAD38.7 cells. The pgRNA/3.5 knt RNA accumulation by Tet removal was monitored in the presence of 5 μg/mL ActD for up to 12 hrs in NMD-depleted HepAD38.7 cells. Two NMD inhibitors, cycloheximide at 100 μg/mL and wortmannin at 20 μM, were also added to the medium at 4 hrs post-ActD treatment. After additional incubation for 8 hrs, the cells were collected to prepare the total RNA for RT-qPCR. Either GAPDH mRNA or 18S rRNA was quantified and the pgRNA/3.5 knt RNA expression level was calculated by the ΔΔCt method relative to the levels of either GAPDH mRNA or 18S RNA.

Western blotting

Cells were harvested and lysed in 2 × SDS sample buffer (125 mM Tris-HCl pH 6.8, 20% glycerol, 4% sodium dodecyl sulfate (SDS), 5% 2-mercaptoethanol and 0.2 mg/mL bromo phenol blue). The lysed protein samples were boiled. The samples were separated by sodium dodecyl sulfate polyacrylamide gel electrophoresis (SDS-PAGE) and transferred to a polyvinyl difluoride (PVDF) membrane (Immuno-Blot PVDF; BioRad). After blocking with 5% dry milk (Nacalai Tesque) containing TBS-T (20 mM Tris-HCl pH 7.6, 150 mM NaCl, and 0.05% Tween20) for 30 min, the membrane was incubated with an appropriate primary antibody overnight at 4°C and subsequently probed with secondary anti-mouse or anti-rabbit IgG conjugated with horseradish peroxidase (HRP) (Dako). After washing with TBS-T at least three times, chemiluminescence was generated by using SuperSignal West Pico Chemiluminescence Substrate (Thermo Fisher Scientific). The image was obtained, and the protein band intensity was measured with an imaging system (ChemiDoc Touch MP or VersaDoc; BioRad).

RNA extraction and Northern blotting

Total RNA from cells was isolated with TRIzol®, and followed by a Direct-zol RNA Miniprep Kit (Zymo Research) or phenol/chloroform extraction according to the manufacturer's instructions. Total RNAs from NMD-depleted HepAD38.7 cells were collected at 0, 4 and 8 hrs after Tet addition. Then, the RNA was treated with DNase I to degrade contaminated DNA. Twenty μg or 5 μg of total RNA was electrophoresed in 1.2% agarose gel under a denatured condition to detect HBV-related transcripts and GAPDH mRNA, respectively. After blotting on a positively charged membrane (GE Healthcare Japan) followed by UV crosslinking, the membrane was probed by either DIG-labeled RNA probes, corresponding to the X region (1374nt to 1838nt) of the HBV adr4 genome (Genbank: #LC090200.1) or to nt 792 to 1251 of human GAPDH mRNA (GenBank: #NM_002046.7). These RNA probes were generated from pSPT18-HBV RNA and pSPT18-hGAPDH, respectively, using DIG RNA labeling kit (Roche) along with manufacture's protocol. The bound probes were reacted with anti-digoxigenin-AP conjugated Fab fragment and the luminescence was generated with CDP-*Star*™ (Roche). The images were obtained with a ChemiDoc™ Touch MP or VersaDoc™ imaging system (BioRad).

HBV-associated DNA/RNA preparation in NMD factor-depleted HepAD38.7 cells and NTCP/G2 cells

The cultured media was collected, and HBV particles were precipitated with 6% polyethylene glycol 8000 overnight at 4°C. The precipitates were suspended in 180 μl of a hypotonic buffer (20 mM Tris-HCl pH 7.6, 50 mM NaCl, 5 mM $MgCl_2$, 5 mM $CaCl_2$, 0.1% 2ME, and 0.1% Nonidet P®-40 (NP®-40)), 10 μl (∼100 Unit) of DNase I (Takara-Clontech) and 5 μl (∼14 μg) of DNase free RNase (Roche Diagnostics). After incubating for 30 min at 37°C and then at 70°C for 30 min, a mixture of 10 μl of 0.25 M EGTA (pH 8.0) and 0.25 M EDTA (pH 8.0) was added to inactivate the DNase I. Then, an equal volume (200 μl) of TE_5 (Tris-HCl pH 7.8, 5 mM EDTA pH 8.0)/1% SDS solution was added, followed by addition of proteinase K (0.2 mg/ml; Roche Diagnostics) and incubation at 56°C overnight. The samples were subjected to DNA extraction using a nucleic acid extraction kit (Maxwell™ RSC Viral TNA; Promega) and an extraction machine (Maxwell™ RSC system; Promega) according to the manufacturer's instruction. For intracellular core-associated HBV DNA, the cells were lysed in 0.4 ml of a hypotonic buffer (20 mM Tris-HCl pH 7.6, 50 mM NaCl, 5 mM $MgCl_2$, 5 mM $CaCl_2$, 0.1% 2ME, and 0.1% Nonidet P®-40 (NP®-40)). The lysate was cleared by centrifugation at 15, 000 × g for 15 min at 4°C and then treated with DNase I and RNase followed by proteinase K, and finally, core-associated HBV DNA was extracted as described above. For intracellular core-associated HBV pgRNA (encapsidated pgRNA), the cleared cell lysate above was treated with DNase I and RNase and TRIzol LS (Thermo Fisher Scientific) was added for RNA isolation according to the manufacturer's instruction.

For cccDNA quantification, at the end of the infection experiment, total genomic DNA of HBV-infected cells were prepared with a Maxwell® RSC genomic DNA kit (Promega). The extracted total DNA was first conducted to digital PCR (dPCR) of RNase P (see below). After measuring the copy number of RNase P by dPCR, all prepared DNA was treated with T5 exonuclease (New England Biolabs) by directly adding 10 units of T5 exonuclease into each tube, followed by incubation for 1 hr at 37°C to degrade genomic and non-completed circular DNA. T5-treated DNA was used for dPCR specific for cccDNA (see below).

RNA-immunoprecipitation (RIP) of HBV RNA

HEK293T cells transfected with IVT-HBV transcripts and HBV-induced HepAD38.7 cells by Tet removal were treated with 500 nM Okadaic acid for 30 min before cell fixation with 0.2% paraformaldehyde/PBS followed by neutralization with 300 nM glycine/PBS. Fixed cells were harvested in RIPA buffer (Nacalai Tesque) containing RNase inhibitor, protease inhibitor and phosphatase inhibitor followed by sonication. The cell extract was incubated with IgG or an anti-pUPF1 antibody at 4°C for 16 hrs with rotation. Then, protein G-conjugated Dynabeads® (Thermo Fisher Scientific) were added and incubated for an additional 4 hrs. The beads were spun down and washed five times with an NT2 buffer (50 mM Tris-HCl, pH7.4, 150 mM NaCl, 1 mM $MgCl_2$, and 0.05% NP®-40). Protein-RNA crosslinks were reversed by heating at 70°C in a buffer (100 mM Tris-HCl, pH 8.0, 10 mM EDTA, 1% SDS, and 2 mM DTT) for 40 min. The bound RNAs with pUPF1 and total RNA as input were recovered by extraction with TRIzol® reagent, followed by RT-qPCR for HBV RNAs, alternative rpL3 mRNA and vtRNA1-1 (see below).

RT-qPCR, qPCR and digital PCR (dPCR)

For RT-qPCR analyses, total RNA in TRIzol® reagent was isolated by a Direct-zol RNA Miniprep Kit (Zymo Research) or phenol/chloroform extraction. The total RNA was reversely transcribed by SuperScript® III transcriptase (Thermo Fisher Scientific) for cDNA synthesis. pgRNA/3.5 knt RNA was quantified with a primer set (HBVpgRNA-qFw and HBVpgRNA-qRv) with a QuantStadio ViiA™ 6 Real-Time PCR Detection System using Fast SYBR™ Green Master Mix (Applied Biosystems). The amount was calculated by the ΔΔCt method relative to levels of GAPDH mRNA, GFP mRNA or 18S RNA. To quantify HBV DNA, core-associated HBV DNA and extracellular HBV DNA were extracted as previously described,[51,52] and the levels of HBV DNA were determined by real-time PCR as described above using the primers HBVDNA-qFw and HBVDNA-qRv. The copy number of HBV DNA was obtained from the standards of serial dilution of pHB I WT. The quantified results were normalized with protein OD to minimize the cell number difference.

Prepared cccDNA was amplified using Absolute Q™ DNA Digital PCR Master Mix (Thermo Fisher Scientific) and QuantStudio Absolute Q (Thermo Fisher Scientific) using primers HBV cccDNA-qFw and HBV cccDNA-qRv and a FAM-MGB probe (HBV cccDNA probe). The RNase P copy number was determined by using a TaqMan™ RNase P Control Reagents Kit (Thermo Fisher Scientific). The cccDNA copy number was normalized with the RNase P copy number, and the data are shown as cccDNA copy number/RNase P copy number.

All the primers for qPCR are listed in Table S1.

Enzyme-linked immunosorbent assay (ELISA)

Levels of HBeAg, HBsAg, PreS1 and PreS2 HBsAg in the culture supernatant or cell lysate were respectively determined by using the following commercial kits: the HBeAg Diagnostic kit (RO Bio), HB S antigen quantitative ELISA kit Rapid-II, HBs PreS-1 antigen quantitative ELISA kit Rapid and HBs PreS-2 antigen quantitative ELISA kit Rapid (Beacle, Inc.).

Immunofluorescence assay

NMD-depleted HEK293T cells were co-transfected with IVT-pgRNA and -GFP mRNA. At 24 hrs post-RNA transfection, the cells were fixed with 1% formaldehyde/PBS and permeabilized by 0.1% TritonX-100/PBS. After blocking with 1% BSA/PBS, GFP and HBc

were probed by a mouse anti-GFP antibody and a rabbit anti-HBc antibody, respectively, then detected by an anti-mouse IgG conjugated with Alexa® 488 and an anti-rabbit IgG conjugated with Alexa® 546 (Thermo Fisher Scientific). The fluorescent signals of GFP and HBc were obtained by ECLIPSE TS2 (Nikon).

NMD reporter assay

NMD-depleted NTCP-HepG2 cells and HepAD38.7 cells were co-transfected with NMD reporter plasmid, pCMV®-globin Norm or pCMV®-globin Ter39, and pCMV®-mMUP using GenJet™ *In Vitro* DNA Transfection Reagent for HepG2 Cells according to the manufacturer's instruction (SignaGen®Laboratories). Also, NTCP-HepG2 cells were co-transfected with an HBV replication plasmid, pCMV®-globin Norm or pCMV®-globin Ter39 and pCMV®-mMUP. At 48 hrs post transfection, the cells were harvested by TRIzol for total RNA isolation, and followed by RT-qPCR using primer sets of NMDGlobin-qFw and NMDGlobin-qRv for detection of globin mRNA, and mMUP-qFw and mMUP-qRv for detection of mMUP mRNA.

QUANTIFICATION AND STATISTICAL ANALYSIS

Statistical analysis

Data were analyzed using one-way or two-way analysis of variance (ANOVA) with appropriate multiple comparisons test using GraphPad PRISM. Details of the statistical tests were specified within the corresponding figure legends, and probability-value differences were considered statistically significant in the following order: $^{*}p < 0.05$, $^{**}p < 0.01$, $^{***}p < 0.005$ and $^{****}p < 0.001$.